Numerical Investigation on Heat Transfer Characteristics of a Triangular Slotted Pin Fin Heat Sink

Rout Jagannath and Yamala Muralikrishna

Nomenclature

a	Size of perforation (mm)
d	Diameter of pin fin (mm)
l_f	Height of fin (mm)
N	Number of fins
N_p	Number of slots
Nu	Nusselt number
p	Pitch of perforations (m)
Re	Reynolds number
T_b	Base temperature of model (K)
Δp	Pressure drop (Pa)
u_i	Inlet velocity of air (m/s)
η	System performance parameter
ρ	Density of air (kg/m^3)

1 Introduction

Thermal execution of perforated pin fin heat sink relies upon different factors, for example, the pitch of aperture and size of puncturing, material properties of the heat

R. Jagannath · Y. Muralikrishna (✉)
Department of Mechanical Engineering, Gayatri Vidya Parishad College of Engineering (Autonomous), Visakhapatnam 530048, A.P., India
e-mail: muralikrishna.yamala@gvpce.ac.in

M. Palanisamy et al. (eds.), *Theoretical, Computational, and Experimental Solutions to Thermo-Fluid Systems*, Lecture Notes in Mechanical Engineering,
https://doi.org/10.1007/978-981-33-4165-4_1

sink. Literature concerning various geometries of heat sinks has been collected, and the details are furnished below. Shaeri et al. [1] examined, numerically, the liquid stream, and conjugate conduction-convective heat transfer from rectangular perforated fins with square windows. The outcomes demonstrate that new perforated fins have higher absolute heat transfer and extensive weight decrease in correlation with solid fins. An experimental and numerical study on finned metal foam and metal foam heat sinks under impinging air jet cooling was carried out by Feng et al. [2]. Fan et al. [3] explored the heat transfer and pressure drop of a novel cylindrical oblique fin heat sink fitted over cylindrical heat sources. Jeng et al. [4] contemplated tentatively heat transfer estimation of the cylindrical heat sink with sintered-metal-bead-layers fins and an implicit motor fan. The study showed that the influence of sintered-bronze-bead layers is negligible in free convection heat transfer. Kim et al. [5] analyzed the thermal performance of optimized plate-fin and pin–fin heat sinks with a vertically situated base plate in natural convection by defining the objective function. Numerical examination on geometric optimization of PCM-based pin fin heat sink is done by Pakrouh et al. [6]. The primary objective of the investigation is to get the designs that augment the heat sink operational time. Singh et al. [7] investigated the heat transfer attributes of an embossed heat sink having rehashed impacts on the fin surface exposed to natural convection. The heat dispersal capacity of the naturally cooled heat sink has been found to be increased by the use of impacts on the fin body. Sajedi et al. [8] broke down numerically the impact of splitter plate on the hydrothermal conduct of pin fin heat sink. To stay away from or debilitate the stream detachment and diminish the pressure drop through the heat sink, a thin plate is situated on the back of the pin. Damook et al. [9] examined utilizing corresponding trial and computational fluid dynamics strategies to find the advantages of utilizing the pin fin heat sinks with different perforations. Li et al. [10] performed numerical examinations on natural convection heat transfer from radial heat sinks with a perforated ring. Shin et al. [11] broke down numerically the qualities of the heat sink with the iconic breeze utilizing wire to parallel plate electrodes utilizing Computational Fluid Dynamics strategy for another cooling gadget of a light-emitting diode. Li et al. [12] examined tentatively the heat transfer of pin fin heat sinks cooled by double piezoelectric fans by infrared thermography. The impacts of the phase difference, the arrangement, the elevation of the piezoelectric fans, and the components of the heat sinks on the thermal performance of the heat sinks are examined. Al-Sallami et al. [13] researched numerically the warm wind currents over strip fin heat sinks utilizing a conjugate heat transfer model; they investigated computationally the advantages of utilizing strip fin heat sinks. Maji et al. [14] explored the heat transfer improvement of heat sink utilizing perforated pin fins with the straight and staggered course of action. Pin fins of different shapes with various perforation geometries to be specific roundabout, diamond-shaped and elliptical sort are considered in their investigation. Their calculations are done by differing inlet speeds, their numerical model is approved with test studies, and great understanding was watched. Ali et al. [15] examined tentatively for the optimization of heat transfer in electronic coordinated circuits utilizing close-packed PCMs filled pin fin heat sinks.

2 Problem Definition and Method of Solution

The present work is proposed to perform numerical heat transfer simulation over a rectangular solid and slotted pin fin heat sink for an inline and staggered fin array. The problem geometry, as shown in Fig. 1, comprises a rectangular base with a fin array protruded from it. Figure 1a–d shows the heat sink with inline slotted fin array, inline solid fin array, staggered slotted fin array, and staggered solid fin array, respectively.

Fins are provided with equilateral triangular slots on their lateral surfaces. A triangular slot offers more surface area than a circular slot for the same cross-section area of the slot. A heat sink is subjected to constant heat flux at its base, and the air is the fluid medium. A heat sink is placed in the fluid stream in such a way that the cross-section of the slot is normal to the direction of flow to ensure that the fluid passes through it.

The equations used for the simulation purpose are the continuity, momentum, and energy equations along with the equations for modeling the quantities of turbulence.

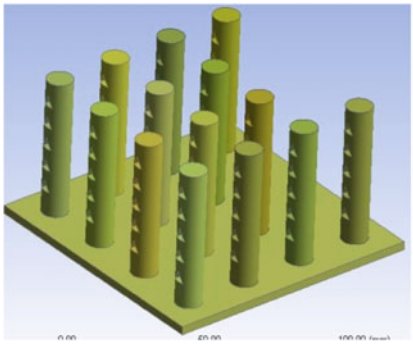

(a) Isometric view of Inline triangular perforated pin fin heat sink

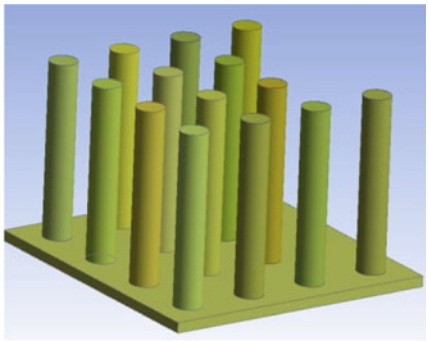

(b) Isometric view of Inline solid pin fin heat sink.

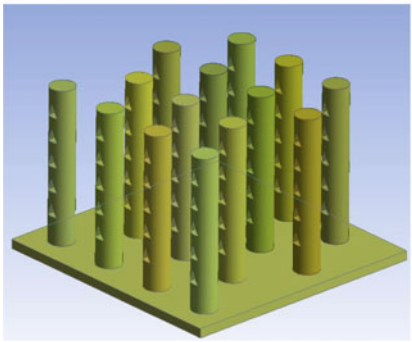

(c) Isometric view of Staggered triangular perforated pin fin heat sink.

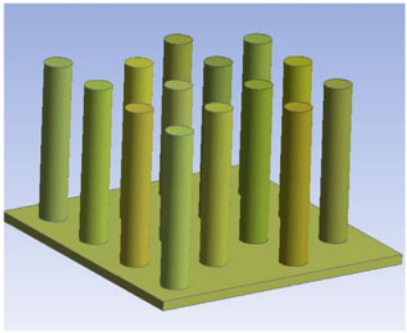

(d) Isometric view of staggered solid pin fin heat sink.

Fig. 1 Rectangular heat sink with slotted pin fin array

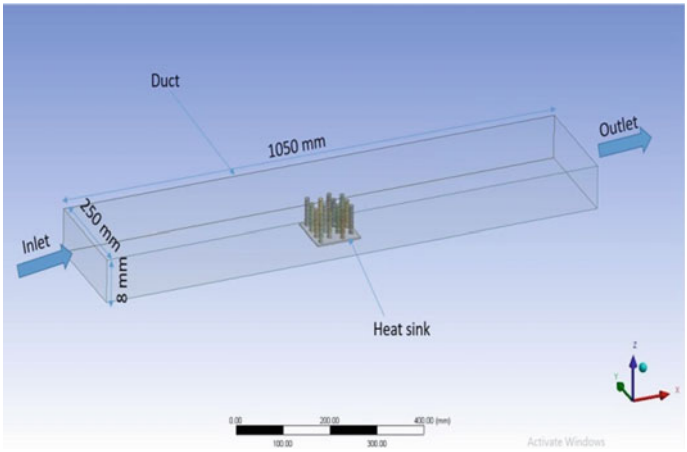

Fig. 2 Computational domain of pin fin heat sink

The assumptions considered in formulating these equations for the current investigations are incompressible flow, no viscous dissipation, steady and buoyancy effects. Standard k- ε model is utilized for the current simulation among a range of turbulence models existing in the ANSYS FLUENT.

Figure 2 shows the computational domain of the present problem, along with the boundary conditions. Airflow passes through the duct inlet, and the heat sink is placed exactly at the mid location of the duct. A heat sink is placed in such a way that the slots are normal to the direction of flow. The base of the heat sink is subjected to constant heat flux, and the remaining walls of the duct are adiabatic and zero heat flux is applied to the four walls of the duct except at the inlet and outlet of the duct. The no-slip wall condition is applied to the four walls of the duct. The boundary condition at the outlet of the duct is applied as pressure outlet conditions.

3 Result and Discussion

3.1 Grid Convergence Test

Grid independence test has been performed on one of the four model models to find the optimum number of elements for the analysis and to reduce the computation time. While doing the grid convergence test, the inlet velocity is taken as 4 m/s, and the applied heat flux is 6000 W/m^2. These values of velocity and heat flux are constant. The test is made by varying the element size by body sizing operation, and results are obtained for the base temperature of the model. Results show that the base temperature of the model decreases with an increase of mesh elements initially and

reaches an asymptotic value for 79,014 number of elements. Therefore, the value is zoned to 79,014 mesh elements, and the computational analysis is carried out.

3.2 Validation of Results

In order to validate the results, the work performed by Maji et al. [14] is considered. A. Maji et al. performed the numerical investigation on a circular slotted pin fin model for both inline and staggered fin array. Convection heat transfer coefficient (h) is taken as a parameter for validating the results. The results of the present work have a decent agreement with benchmark results with a maximum deviation of 13.09%.

3.3 Local Temperature Profiles

Figures 3, 4, 5 and 6 show the local temperature profiles of all four geometries of the heat sink. The present study is made for a fixed input of heat flux, Reynolds number (Re) as shown in Figure. Figure 6 demonstrates that the temperatures along with the fin decrease from base to fin and is maximum at the base. It is evident to note that the local fin temperatures, at any location on the fin, increases in the downstream of flow. The above is true due to a fresh air stream is in contact with the first row. A similar pattern of temperature profiles has been observed for all four heat sink geometries. Further, the local temperatures of the fin, at any given location, for a model with triangular slotted fins are less than that of a solid pin fin model. This is due to an increased rate of convection with slots in fins. For a comparison between inline fin array and staggered fin array, Figs. 3 and 5 show that, the staggered fin array observes

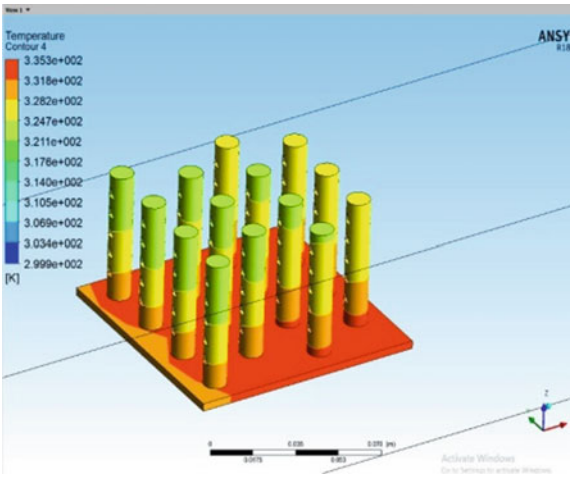

Fig. 3 Temperature distribution of staggered triangular slotted pin fin model

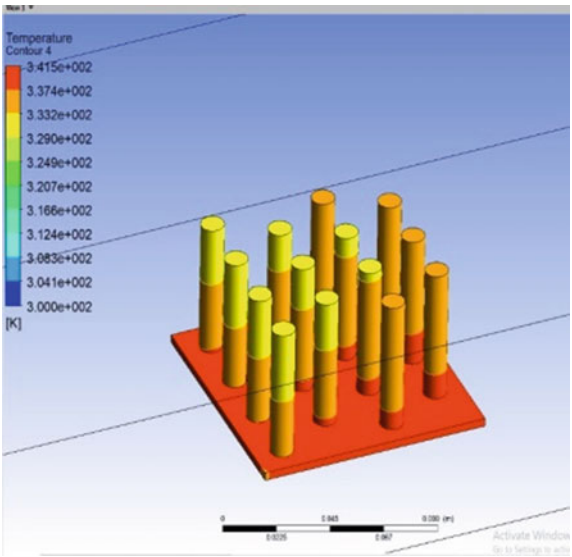

Fig. 4 Temperature distribution of solid staggered pin fin model

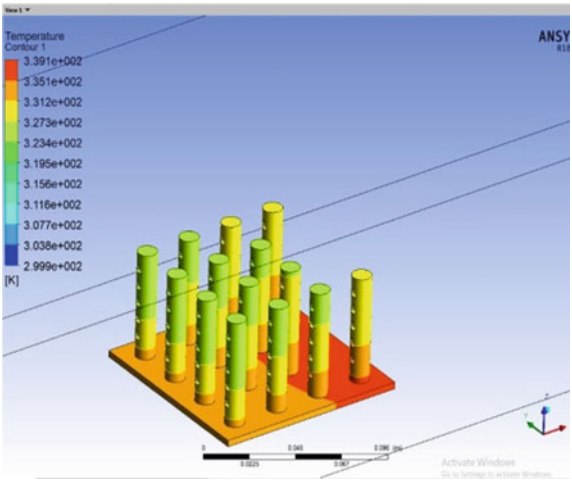

Fig. 5 Temperature distribution of inline triangular slotted pin fin model

low-temperature value than an inline array for the identical location of the fin and on the fin. Because the flow pattern of staggered fin array is more advantageous in comparison to the flow across an inline fin array. The above study concludes that the local heat sink temperatures are less for the triangular slotted pin fin model and are further dropped down by making use of staggered arrangement for fin array.

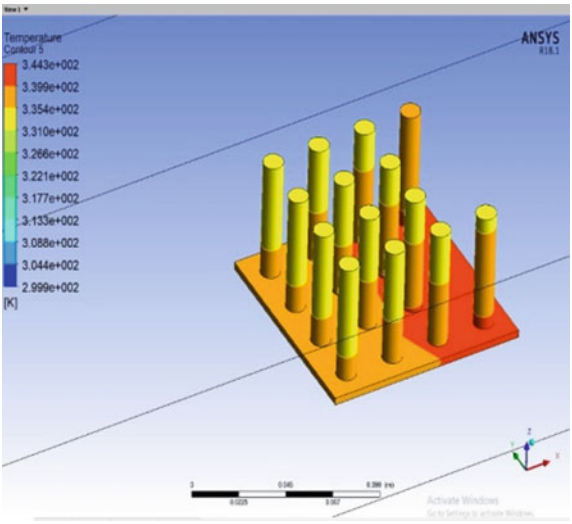

Fig. 6 Temperature distribution of inline solid pin fin model

3.4 Base Temperature of Heat Sink

The following studies are performed to understand the effect of different variables on the base temperature of the heat sink. Investigations have been performed to obtain the results for the base temperature of the heat sink by varying the inlet velocities from 4 to 12 m/s and by keeping the applied heat flux as constant for all the models. Figure 7 demonstrates the variation in the base temperature of the model with the inlet velocity of air for the inline and staggered arrangement for both solid and triangular slotted pin fins. The base temperatures decrease with an increase in velocity due to

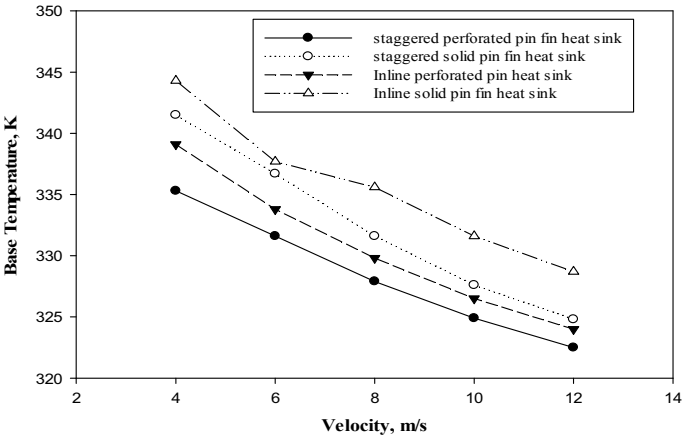

Fig. 7 Base temperature of various models by varying inlet velocity

an increased rate of convective heat dissipation. At all velocities, results show that the base temperature for the triangular slotted pin fin model is lower than that of the solid pin fin model in both the arrangements.

This is due to, an expected, the slots in fins enhances the rate of convective heat dissipation by providing more surface area of contact between the fin and cooling medium. For example, at a flow velocity 6 m/s, for an inline arrangement, the base temperature drops down by 4 °C by providing slots in fins. Further, the base temperature is even tested for two different kinds of fin array, namely (i) inline and (ii) staggered arrangement. Results disclose that the model with staggered fin array experiences less base temperature and is clearly obvious from Fig. 7. This is due to bifurcation of the mainstream at the front leading edge of each pin fin, while, for inline arrangement, most of the fins are in the wake region of preceding cylinders.

3.5 Nusselt Number

Nusselt number (Nu) is a non-dimensional convective heat flux that depends on flow properties, fluid properties and flow geometry. The following study has been made to outline the variation of Nusselt number with flow geometry for different flow velocities. Figure 8 describes the variation in Nusselt number of the model with the Reynolds number for an inline and staggered arrangement for both solid and slotted pin–fin models. For any given geometry, the Reynolds number is varied from 27,056 to 81,168 by keeping heat flux constant at 6000 W/m^2. The Nusselt number increases with the increase in Reynolds number due to the increased rate of convective heat transfer. At all Reynolds number, results show that the Nusselt number for the triangular slotted pin fin model is higher than that of the solid pin fin

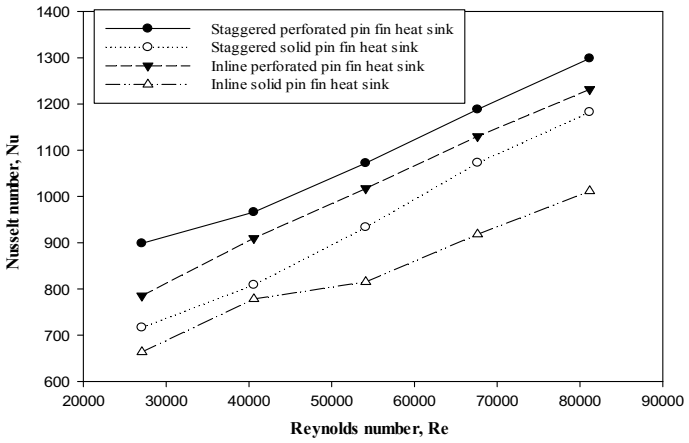

Fig. 8 Nusselt number of various models by varying Reynolds number

model in both the arrangements. Because, the slots provided in the fins, increase the apparent surface area for convective heat dissipation. A 35.38% increase in Nusselt number is observed by replacing an inline solid fin array with a staggered triangular slotted fin array.

3.6 Pressure Drop Across the Heat Sink

In fluid dynamics, it is equally important to estimate the pressure drop along with the Nusselt number. Because pressure drop (Δp) helps in determining the pumping power requirement. In most of the ones, the increased convective heat transfer, that is, increased Nusselt number, is always associated with increased pressure drop which demands more pumping power. So, in order to estimate the pressure drop across the heat sink with varying Reynolds number, the results are obtained. Figure 9 demonstrates the variation in pressure drop of the model with the Reynolds number for an inline and staggered arrangement for both solid and triangular slotted pin fin models. The pressure drop increases with an increase in Reynolds number and attains its highest value in the case of solid fins because the solid fins provide more obstruction to fluid flow than triangular slotted pin fins. At all Reynolds number, results show that the pressure drop for the solid pin fin model is higher than that of the triangular slotted pin fin model in both the arrangements. Substantial pressure drops have been observed by making use of a triangular slotted pin fin heat sink. For example, the pressure losses are 66.6% lower with an inline triangular slotted pin–fin arrangement in comparison to that of staggered solid pin fin array.

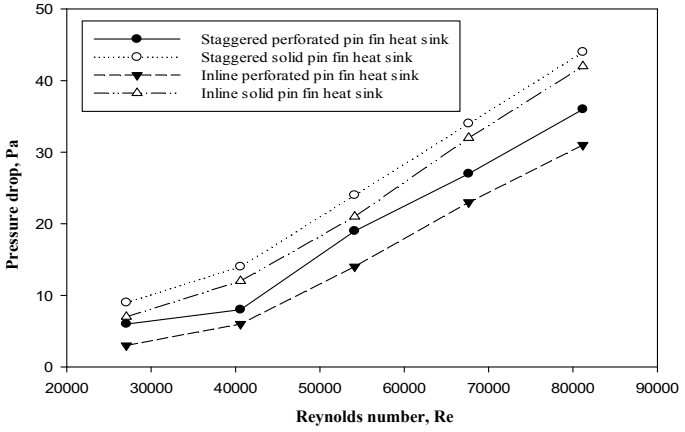

Fig. 9 Pressure drops of various models at different Reynolds number

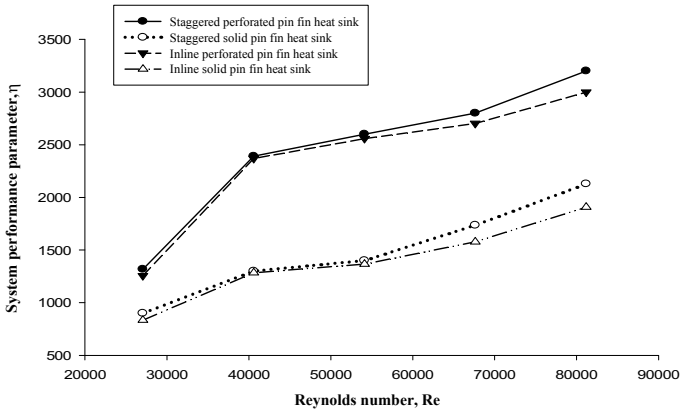

Fig. 10 System performance parameter of various models at different Reynolds number

3.7 Thermal Performance of Heat Sink

The thermal performance parameter (η) of the heat sink is defined as the ratio of the Nusselt number to the skin friction coefficient of the model. It signifies relative dominance of convective heat dissipation over the associated pressure drop, that is, pumping power requirements. Figure 10 depicts the variation in thermal performance parameter with Reynolds number for an inline and staggered arrangement for both solid and triangular slotted pin fin model geometries. The thermal performance parameter increases with an increase in Reynolds number due to an increased rate of thermal dissipation. At all Reynolds number, results show that the system performance parameter for the triangular slotted pin fin model is higher than that of the solid pin fin model in both the arrangements. This is due to that the slots in fins increase convection heat transfer in one way and reduces the pressure losses, and thus the pumping power required on the other way. The thermal performance of the system was enhanced by 57.9% with a staggered triangular slotted pin–fin arrangement in place of an inline solid pin–fin array. From the above results, it is evident that the Nusselt number for staggered triangular slotted pin fin model is best, and the pressure drop for an inline triangular slotted pin fin model is low. So to obtain the overall best configuration, the system performance parameter is used. In addition, the graph shows that the staggered triangular slotted pin fin model is best among all the models.

4 Conclusions

A numerical investigation over a triangular slotted pin fin and solid pin fin model with inline and staggered arrangement by varying inlet velocities has been made.

The results are validated for the convective heat transfer coefficient with benchmark solutions Maji et al. [14] and found to be in decent agreement with a maximum percentage of deviation of 13.09%. The average heat sink temperature is less for the triangular slotted pin fin model in comparison with the solid pin fin model and is further less in staggered arrangement. The maximum temperature of the heat sink, base temperature, is 9 °C less with a staggered triangular slotted pin–fin arrangement in comparison to that of inline solid pin fin array. The Nusselt number of staggered arrangement is more than that of inline arrangement at any given Reynolds number. Further, the triangular slotted pin fin model observes a high Nusselt number in comparison to that of the solid pin fin model. A 35.38% increase in Nusselt number is observed by replacing an inline solid fin array with a staggered triangular slotted fin array. The substantial drop in pressure losses has been observed with a triangular slotted fin. A 66.6% drop in pressure loss is achieved with a triangular slotted pin fin model in comparison to that of a solid pin fin model. The thermal performance parameter is 57.9% higher with a staggered triangular slotted pin–fin arrangement in place of inline solid pin fin array.

References

1. Shaeri MR, Yaghoubi M, Jafarpur K (2009) Heat transfer analysis of lateral equilateral triangular slotted fin models. Appl Energy 86:2019–2029
2. Feng SS, Kuang JJ, Wen T, Lu TJ, Ichimiya K (2014) An experimental and numerical study of finned metal foam models under impinging air jet cooling. Int J Heat Mass Transf 77:1063–1074
3. Fan Y, Lee P, Jin L-W, Chua B (2014) Experimental investigation on heat transfer and pressure drop of a novel cylindrical oblique fin model. Int J Therm Sci 76:1–10
4. Jeng T-M, Tzeng S-C (2014) Heat transfer measurement of the cylindrical model with sintered-metal-bead-layers fins and a built-in motor fan. Int Commun Heat Mass Transf 59:136–142
5. Joo Y, Kim SJ (2015) Comparison of thermal performance between plate-fin and pin-fin models in natural convection. Int J Heat Mass Transfer 83:345–356
6. Pakrouh R, Hosseini MJ, Ranjbar AA, Bahrampoury R (2015) A numerical method for PCM-based pin fin models optimization. Energy Convers Manage 103:542–552
7. Singh P, Patil AK (2015) Experimental investigation of heat transfer enhancement through embossed fin model under natural convection. Exp Thermal Fluid Sci 61:24–33
8. Sajedi R, Osanloo B, Talati F, Taghilou M (2016) Splitter plate application on the circular and square pin fin models. Microelectron Reliab 62:91–101
9. Al-Damook A, Kapur N, Summers JL, Thompson HM (2015) An experimental and computational investigation of thermal air flows through equilateral triangular slotted pin models. Appli Thermal Eng 89:365–376
10. Li B, Jeon S, Byon C (2016) Investigation of natural convection heat transfer around a radial model with a equilateral triangular slotted ring. Int J Heat Mass Transf 97:705–711
11. Shin DH, Baek SH, Ko HS (2016) Development of model with ionic wind for LED cooling. Int J Heat Mass Transf 93:516–528
12. Li H-Y, Wu Y-X (2016) Heat transfer characteristics of pin-fin models cooled by dual piezoelectric fans. Int J Therm Sci 110:26–35
13. Al-Sallami W, Al-Damook A, Thompson HM (2016) A numerical investigation of thermal airflows over strip fin models. Int Commun Heat Mass Transf 75:183–191
14. Maji A, Bhanja D, Patowari P (2017) Numerical investigation on heat transfer enhancement of model using equilateral triangular slotted pin fins with inline and staggered arrangement. Appl Therm Eng 125:596–616

15. Ali HM, Ashraf MJ, Giovannelli A, Irfan M, Irshad TB, Hamid HM, Hassan F, Arshad A (2018) Thermal management of electronics: an experimental analysis of triangular, rectangular and circular pin-fin models for various PCM's. Int J Heat Mass Transf 123:272–284